Per-Pixel Water and Oil Detection on Surfaces with Unknown Reflectance

Chao Wang
Department of Artificial Intelligence
Kyushu Institute of Technology
Iizuka, Japan
c_wang@pluto.ai.kyutech.ac.jp

Takahiro Okabe
Department of Artificial Intelligence
Kyushu Institute of Technology
Iizuka, Japan
okabe@ai.kyutech.ac.jp

***Abstract*—Water and oil detection is important for machine vision applications such as visual inspection and robot motion planning. It is known that water absorbs near infrared light and oil absorbs near ultraviolet and blue light. Therefore, observing at the absorbed wavelengths, the apparent spectral reflectances of surfaces with water/oil are smaller than that without water/oil. We could detect water/oil based on the above absorption features by using a hyperspectral image, if the original spectral reflectances of surfaces are known. However, in general, the spectral reflectances of surfaces are unknown and spatially varying. In this paper, we propose a novel per-pixel water and oil detection method based on the Lambert-Beer's law and a low-dimensional linear model for spectral reflectance. We show that our method enables us to pixelwisely detect water and oil on surfaces with unknown and spatially-varying reflectance at high accuracy by using a hyperspectral image. The effectiveness of our proposed method is confirmed through a number of experiments using real hyperspectral images.**

***Index Terms*—water and oil detection, absorption, hyperspectral imaging, spectral reflectance**

I. Introduction

Detecting water and oil on object surfaces such as road surfaces, floors, and manufactured products in a non-contact and non-destructive manner is vital to applications for autonomous driving systems, robot path planning [1], and visual inspection [2], [3]. In spite of its importance, water and oil detection has received little attention in image processing literature.

Image-based water and oil detection is a challenging problem. As shown in Fig.1 (a) and (b), water/oil is transparent/translucent for visible wavelengths, and then the appearance of water/oil on object surfaces significantly depends not only on water/oil themselves but also on the background object surface. Therefore, it is difficult to distinguish surfaces with/without water/oil from ordinary color images.

Interestingly, it is known that water absorbs near infrared (NIR) light, and oil absorbs near ultraviolet (NUV) and blue light. Therefore, observing at those wavelengths, the brightness of an object surface on which water/oil is present is smaller than that without water/oil, because NIR/NUV light, incoming to and outgoing from the object surface, is absorbed by water/oil. In other words, the *apparent* spectral reflectance, *i.e.* the ratio between the spectral radiance observed at a surface point and the spectral irradiance, is smaller when

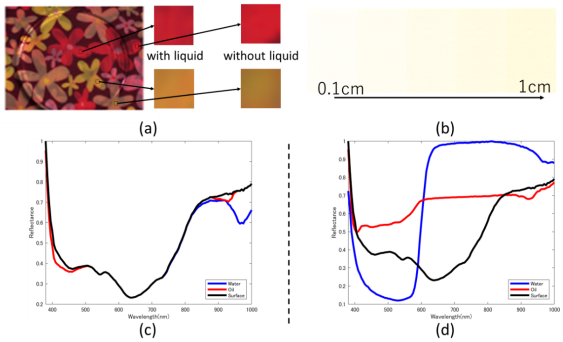

Fig. 1. (a) The scene of an object surface with water (the reflectances are converted into an RGB image). The first column is pixels with water, and the second column is pixels without water. (b) The apparent reflectances (shown by RGB image) of a white background with oil with different thicknesses from 0.1cm to 1cm. (c) and (d) are two cases of water and oil detection. One is that the surface with known spectral reflectance as shown in (c), and another is that the surface with unknown and spatially varying spectral reflectance (for example, three points on the surface with different spectral reflectance) as shown in (d). The black lines are the surface original reflectance, the blue lines are the surface with water apparent reflectance, and the red lines are the surface with oil apparent reflectance.

water/oil is present. Hence, we could detect water/oil by using hyperspectral image if the *original* spectral reflectance of object surfaces is known (as shown in Fig.1 (c)).

However, the *original* spectral reflectances of object surfaces are unknown and spatially varying in general. Therefore, when the *apparent* spectral reflectance of object surfaces is small, we cannot distinguish two possible cases: one is that the *original* spectral reflectance itself is small, and another is that the *apparent* spectral reflectance is small due to the absorption by water/oil (as shown in Fig.1 (d)).

Accordingly, in this paper, we propose a method for per-pixel water and oil detection via hyperspectral imaging. Specifically, based on the Lambert-Beer's law [4], our proposed method estimates the original spectral reflectance and liquid thickness at each surface point from its apparent spectral reflectance simultaneously. First, we make use of the low-dimensional linear combination model for spectral reflectance from visible to NIR wavelengths. Then, water and oil are detected on the basis of the loss between the apparent spectral reflectance computed by using the estimated spectral reflectance, absorption coefficient, and estimated liquid thick-

ness, and the observed apparent reflectance. To demonstrate the effectiveness of our method, we conducted a number of experiments using real images. We also compared the performance of the low-dimensional linear model for spectral reflectance reconstruction with sparse representation [5].

In summary, our main contributions are twofold. First, we propose a novel method to simultaneously estimates the original spectral reflectance and liquid thickness at each surface point simultaneously from a single hyperspectral image. Our method enables us to detect water and oil on surfaces with unknown and spatially-varying reflectance. To our knowledge, ours is the first water and oil detection on object surfaces with unknown spectral reflectance. Second, we compared the low-dimensional linear model for spectral reflectance reconstruction with sparse representation to show which model is more suitable for our water and oil detection method.

II. Related Work

Water Detection: In general, static water has sky reflection outdoors, and then the area of water with sky reflection can be easily distinguished from other terrains by brightness [6], [7]. These aforementioned approaches are all promising but the scene in which the above method can be applied is limited. Especially, surfaces with unknown and spatially-varying reflectance, its brightness also spatially-varying, thus difficult to detect water. In recent years, using LDA [8] for classific different colors of water and different backgrounds. Nevertheless, it affected by the liquid thickness leads to obtaining undesired results. In contrast to the above methods, our method enables us to detect water and oil with unknown thicknesses on surfaces with unknown and spatially-varying reflectance. Wang et al. [9] estimate the original NIR reflectance from the visible reflectance to detect water. The difficulty of water and oil detection is that we cannot estimate the original spectral reflectance from the reflectance in visible range because oil absorbs a part of visible light. Our proposed method can estimate the physical parameters such as optical path length as well as the presence/absence of water/oil.

Oil Detection: In remote sensing literature, Salem et al. [10] proposed an oil spill detection method by using hyperspectral images in the early years. In recent years, Pabon et al. [11] have proposed a method based on diffuse reflection to detect oil-contaminated soil. Menezes et al [12] and Liu et al. [13] have proposed methods to detect different types of oil spills. Achard et al. [14] use spectral image unmixing in order to extract training samples and then apply SVM to detect onshore hydrocarbon. On the other hand, in food safety literature, PCA is used to analyze spectral data to identify whether oil is adulterated [15]. However, the above methods assume known background (sea etc.) and require special experimental equipments (test tube etc.). Therefore, they cannot detect oil (and water) on surfaces with unknown and spatially-varying reflectance without using special equipments.

Lambert Beer's Law: Attenuation due to light absorption is described by the Lambert-Beer's law [4] and has been used for water depth estimation [16] and powder detection [17]. Asano et al. [16] proposed a method of estimating the depth of objects in water based on the multi-wavelength image using the fact that water absorbs NIR light. Zhi et al. [17] proposed a method for powder recognition using multi-spectral imaging. They use the lambert-Beer's law to modeling powders. In contrast to this approach, our method uses the Lambert-Beer's law to estimates the original spectral reflectance and liquid thickness at each surface point from its apparent spectral reflectance.

Low-Dimensional Linear Model for Spectral Reflectance Reconstruction: Parkkinen et al. [18] measured and analyzed the spectral reflectance of the Munsell Color Book and showed that the visible spectral reflectance in the visible light can be approximated by a linear combination of a small number of basis vectors. Wang et al. [9] extend Parkkinen et al. method from visible wavelengths to NIR wavelengths. In recent years, the low-dimensional linear model has been widely used to reconstruct the spectral reflectance [19]–[23]. Compared with the above method, we apply it to the detection of water and oil per pixel.

III. Proposed Method

A. Apparent Spectral Reflectance

We capture an image of a scene of interest by using a hyperspectral camera. Suppose that the spectral irradiance of the scene is uniform and known up to per-pixel scale, i.e. the scene is illuminated by a single light source or multiple light sources with the same SPD (spectral power distribution). The per-pixel spectral irradiance can be measured up to a scale by taking a hyperspectral image of the scene and the white balance and diffuse reflectance target of Spectralon at the same time for example.

We denote the spectral radiance and irradiance at a certain surface point by $S(\lambda)$ and $L(\lambda)$ respectively. Then, we express the reflectance at the surface point based on the Lambert-Beer's law [4]. Given wavelength λ, the Lambert-Beer law accurately expresses light absorption as the relation between radiance $S(\lambda)$ and irradiance $L(\lambda)$,

$$S(\lambda) = \rho(\lambda)L(\lambda)e^{-\alpha(\lambda)l} \tag{1}$$

in which $\rho(\lambda)$ represents the original spectral reflectance of the surface, l represents liquid thickness (optical path length), and $\alpha(\lambda)$ denotes the spectral absorption coefficient.

Therefore, the apparent spectral reflectance $\hat{\rho}(\lambda)$ at the surface point is given by[1]

$$\hat{\rho}(\lambda) = \frac{S(\lambda)}{L(\lambda)} = \rho(\lambda)e^{-\alpha(\lambda)l}. \tag{2}$$

The apparent spectral reflectance is determined by the surface original spectral reflectance, spectral absorption coefficient, and liquid thickness.

[1]We determine the scale of the apparent spectral reflectance so that its maximum value with respect to λ is 1 without loss of generality.

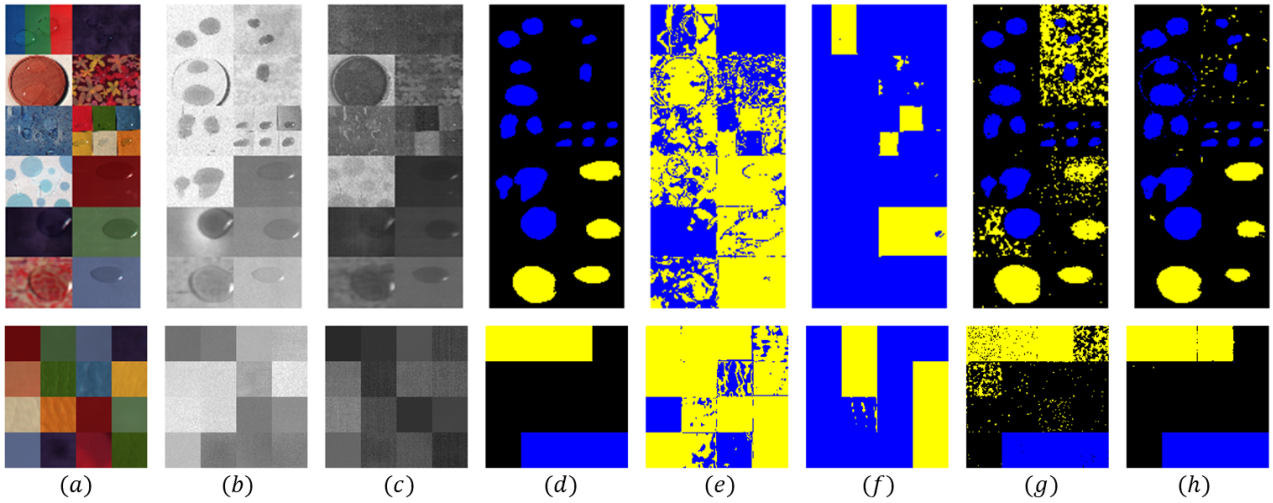

Fig. 2. The experimental results : (a) Pseudo RGB image, (b) 400nm image, and (c) 975nm image of the scene where water and oil are present. (d) Correct label: with water (blue), with oil (yellow), background (black). Detection results: (e) RGB L1sparse, (f) RGB PCA, (g) HSI L1sparse, (h) HSI proposed (our proposed method)

B. Low-Dimensional Linear Model for Spectral Reflectance

Parkkinen *et al.* [18] studied the spectral reflectances of the Munsell Color Book chips, and showed that the spectral reflectances in visible wavelengths are approximately represented by linear combinations of the basis functions derived via Principal Component Analysis (PCA) [24]. Specifically, a spectral reflectance $\rho(\lambda)$ is represented as

$$\rho(\lambda) \simeq \sum_{n=1}^{N} c_n b_n(\lambda), \tag{3}$$

where λ stands for the wavelength of incoming and outgoing light, and $b_n(\lambda)$ and c_n are the n-th basis function ($n = 1, 2, 3, ..., N$) and its coefficient respectively.

Recently, Wang *et al.* [9] experimentally show that the low-dimensional linear model in eq.(3) is applicable not only to visible wavelengths but also to visible to NIR wavelengths. In this paper, our proposed method uses the low-dimensional linear model from visible to NIR wavelengths.

C. Per-Pixel Water and Oil Detection

We assume that the spectral absorption coefficients of water and oil are known, and the absorption coefficient of none is 0. Our proposed method detects water and oil per pixel by estimating the liquid types (water or oil or none), the original spectral reflectance and liquid thickness at each surface point simultaneously from its apparent spectral reflectance. Specifically, substituting Eq.(3) into Eq.(2), the apparent spectral reflectance can be approximated by

$$\tilde{\rho}(\lambda) = \left[\sum_{n=1}^{N} c_n b_n(\lambda)\right] e^{-\alpha(\lambda) l}. \tag{4}$$

Here, $\tilde{\rho}(\lambda)$is approximated apparent spectral reflectance. The coupling coefficient c_n is estimated for each pixel so that the spectral reflectance is non-negative. Then, our method minimizes the squared error between $\tilde{\rho}(\lambda)$ and $\hat{\rho}(\lambda)$ as

$$\min_{\{c_n, \alpha(\lambda), l\}} \int (\tilde{\rho}(\lambda) - \hat{\rho}(\lambda))^2 d\lambda. \tag{5}$$

Specifically, we estimate the liquid type (water or oil or none) and the liquid thickness discretely, and estimate the surface spectral reflectance coefficient continuously. We fix the liquid types (water or oil or none) and the liquid thickness, solve the spectral reflectance by the constrained least square method. And perform the above calculation while changing the liquid types (water or oil or none), and the liquid thickness. In particular, the absorption coefficient $\alpha(\lambda)$ is from three types of water, oil, and none, and the thickness l is in the range of 0 mm to 10 mm, and the step size is 0.1 mm.

In addition, as a comparison method, we compare the effect of sparse representation [5] in detecting water and oil. We use Munsell Color Book chips reflectances as a dictionary for representing spectral reflectance. Here, the apparent spectral reflectance can be approximated by

$$\min_{\{W, \alpha(\lambda), l\}} ||\tilde{\rho}(\lambda) - WDe^{-\alpha(\lambda) l}||^2 + k||W||_1, \tag{6}$$

where we define the sparse coefficient matrix as W, the color chips dictionary matrix as D, and k as a sparse parameter.

IV. Experiments

A. Water and Oil Detection

In the experiment, object surfaces were illuminated by a halogen lamp, and a hyperspectral camera manufactured by EBA JAPAN was used. We sampled spectral reflectances from 380 to 1000 nm at 5-nm intervals, and then obtained 125 bands of hyperspectral images. In this paper, the spectral irradiance of the scene is measured by using a standard diffuse reflector. Then, the apparent spectral reflectances were obtained by dividing the spectral radiances by the measured spectral irradiance.

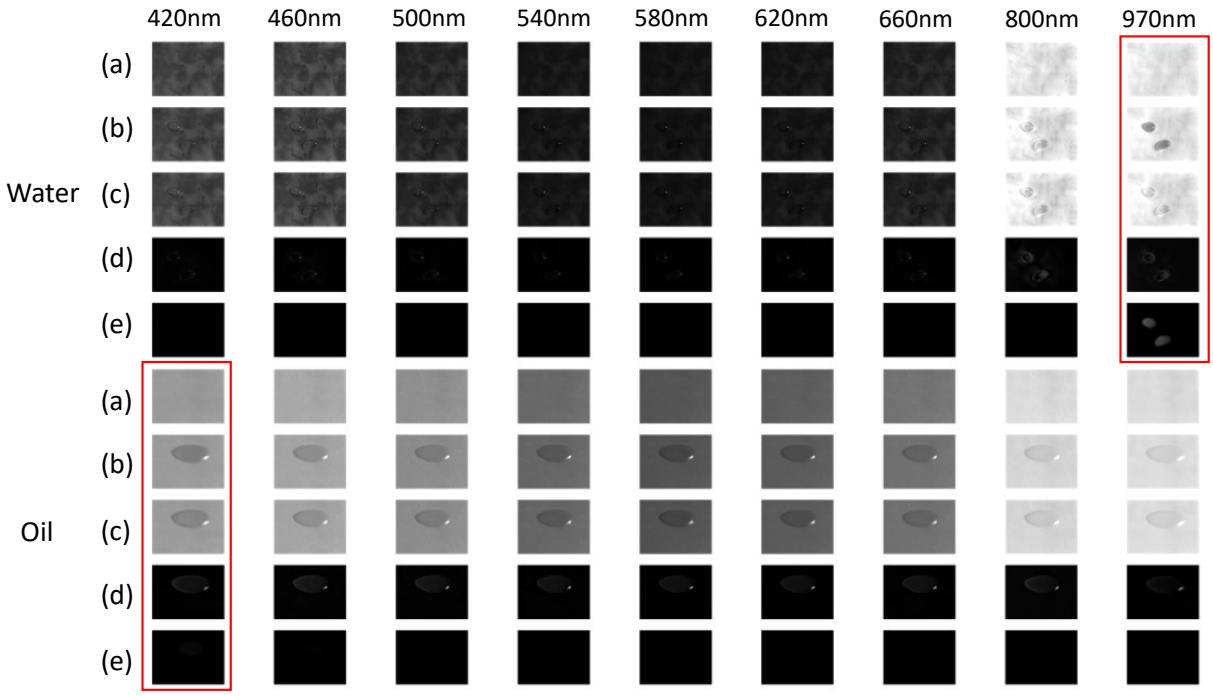

Fig. 3. (a) The original reflectance of the surface. (b) The apparent spectral reflectance of the liquid (water and oil) on the surface. (c) The reconstructed reflectance of the proposed method. (d) The RMSE between the reconstructed reflectance and the original reflectance. (e) RMSE between reconstructed reflectance and apparent spectral reflectance.

We tested the performance of water and oil detection on 17 surfaces; 4 cloths with complex texture, 3 floor tiles with uniform colors, 3 pieces of paper with different colors, 6 pieces of leather with different colors, 1 wood, and 1 mixed scene (consisting of 5 different materials with 16 different colors). In order to obtain the ground truth labels for quantitative analysis, we first captured the image of the object surface without water/oil, and then captured the image of the object surface with water/oil, and applied the active contour method [25] to their subtraction. The following comparisons are conducted to show the effectiveness of the hyperspectral image and the low-dimensional linear model.

RGB L1sparse: We use the RGB apparent reflectance generated by assuming Canon EOS-1D Mark III's spectral sensitivity [26] as the input data, and approximate the RGB apparent reflectance based on the sparse representation [5]. Here, we set the range of the sparse parameter k in eq.(6) to be between 1 and 10, and select the optimal value that yields the largest mFscore as a comparison for our method.

RGB PCA: We use the RGB apparent reflectance generated by assuming Canon EOS-1D Mark III's spectral sensitivity [26] as the input data, and approximate the RGB apparent reflectance based on the low-dimensional linear model with PCA [24]. Here, the number of basis functions is 2.

HSI L1sparse: We use the apparent spectral reflectance captured by a hyperspectral camera as the input image, and we approximate the apparent spectral reflectance based on the sparse representation [5]. Here, we set the range of the sparse parameter k in eq.(6) to be between 1 and 10, and select the optimal value that yields the largest mFscore as a comparison for our method.

TABLE I
RESULTS FOR METHOD PERFORMANCE.

Method	mPrecision	mRecall	mFscore
RGB L1sparse	0.1288	0.4549	0.2008
RGB PCA	0.1050	0.3475	0.1612
HSI L1sparse	0.8620	0.9326	0.8960
HSI proposed	**0.9706**	**0.9768**	**0.9737**

First, in Fig. 2(a)-(d), we show are the Pseudo RGB image, the 400nm image, the 975nm image of the scene where water and oil are present, and the label, from left to right. We can see that water and oil detection based on the RGB image or the absorption band image is difficult.

Second, the results of RGB L1sparse and RGB PCA are shown in Fig. 2(e)(f) show that RGB images do not work well no matter whether the low-dimensional linear model and sparse representation, effective results cannot be obtained. This is because water is transparent under visible light and the apparent spectral reflectance is the same as surfaces spectral reflectance. In addition, the experimental result shows that it is difficult to detect oil when using RGB images because the absorption of blue wavelengths is small.

Third, in Fig. 2(g), we show the sparse representation result, which uses a small number of spectral reflectance to approximate the apparent spectral reflectance. In Fig. 2(h), compared with the above methods, our proposed method has obtained robust results.

Table I shows the results of quantitative evaluation. Three indexes, mRecall, mPrecision and mFscore, were used for

quantitative analysis. They represent average recall, average precision, and average Fscores for water, oil, and background detection. The mFscores of RGB L1sparse and RGB PCA methods are very low. In addition, in the HSI L1sparse, the apparent spectral reflectance is approximated based on a small number of Munsell Color Book data. If the sparse parameter k is small, the result will be affected by noise, otherwise, it will reduce the data used and make approximation difficult. Therefore, we chose the k that obtains the best mFsorce as a comparison. The experimental result shows that our method performs better than the above methods.

B. Spectral Reconstruction

Our water and oil detection method is based on the estimation of the liquid thickness and surface spectral reflectance from a hyperspectral image. It is very interesting that we have obtained the reconstruction of surface spectral reflectance as an intermediate product while detecting water and oil.

The results are shown in Fig. 3. We choose the root mean square error (RMSE) as our evaluation metric. We calculate the RMSE between the reconstructed spectral reflectance and the surface original spectral reflectance as shown in Fig. 3(d) and the RMSE between the reconstructed spectral reflectance and the surface apparent spectral reflectance as shown in Fig. 3(e). The result show that our spectral reconstruction is effective. In particular, the absorption wavelength result (framed in red in the Fig. 3), shows that the surface texture under the liquid is clearly reconstructed.

Because we can estimate the liquid type and the surface reflectance reconstruction, we can edit the apparent spectral reflectance by changing any element in the eq.(2). In addition, it is also very helpful for surface classification applications when we do not know whether there is liquid on the surface.

V. Conclusion and Future Work

In this paper, we proposed a method for per-pixel water and oil detection on surfaces with unknown and spatially-varying reflectance. Based on the Lambert-Beer ' s law and a low-dimensional linear model for spectral reflectance, water and oil are detected on the basis of the loss between the apparent spectral reflectance computed by using the estimated spectral reflectance, absorption coefficient, estimated liquid thickness, and the observed apparent reflectance. We conducted a number of experiments using real images, and confirmed that our proposed method performs well. In the future, we will reduce the number of bands to design a simple camera for water and oil detection.

Acknowledgment

This work was supported by JSPS KAKENHI Grant Numbers JP17H01766 and JP20H00612.

References

[1] B. Ichter, J. Harrison, and M. Pavone, "Learning sampling distributions for robot motion planning," in *Proc. IEEE ICRA 2018*, 2018, pp. 7087–7094.

[2] F. Pernkopf and P. O'Leary, "Image acquisition techniques for automatic visual inspection of metallic surfaces," *NDT & E International*, Vol. 36, No. 8, pp. 609–617, 2003.

[3] S. Agnisarman, S. Lopes, K. Madathil, K. Piratla, and A. Gramopadhye, "A survey of automation-enabled human-in-the-loop systems for infrastructure visual inspection," *Automation in Construction*, Vol. 97, pp. 52–76, 2019.

[4] A. Beer and P. Beer, "Determination of the absorption of red light in colored liquids," *Annalen der Physik und Chemie*, Vol. 86, No. 5, pp. 78–88, 1852.

[5] R. Tibshirani, "Regression shrinkage and selection via the lasso," *Journal of the Royal Statistical Society: Series B (Methodological)*, Vol. 58, No. 1, pp. 267–288, 1996.

[6] A. Rankin and L. Matthies, "Daytime water detection based on color variation," in *Proc. IEEE/RSJ IROS 2010*, 2010, pp. 215–221.

[7] A. Rankin, L. Matthies, and P. Bellutta, "Daytime water detection based on sky reflections," in *Proc. IEEE ICRA 2011*, 2011, pp. 5329–5336.

[8] A. Fisher, N. Flood, and T. Danaher, "Comparing landsat water index methods for automated water classification in eastern australia," *Remote Sensing of Environment*, Vol. 175, pp. 167–182, 2016.

[9] C. Wang, M. Okuyama, R. Matsuoka, and T. Okabe, "Per-pixel water detection on surfaces with unknown reflectance," to appear in the IEICE Transactions on Information and Systems.

[10] F. Salem, M. Kafatos, T. El-Ghazawi, R. Gomez, and R. Yang, "Hyperspectral image analysis for oil spill detection," in *Summaries of NASA/JPL Airborne Earth Science Workshop, Pasadena, CA*, 2001, pp. 5–9.

[11] R. Pabón, C. De Souza Filho, and W. De Oliveira, "Reflectance and imaging spectroscopy applied to detection of petroleum hydrocarbon pollution in bare soils," *Science of the Total Environment*, Vol. 649, pp. 1224–1236, 2019.

[12] J. Menezes and N. Poojary, "A fusion approach to classify hyperspectral oil spill data," *Multimedia Tools and Applications*, Vol. 79, No. 7, pp. 5399–5418, 2020.

[13] B. Liu, Y. Li, Q. Zhang, and L. Han, "Assessing sensitivity of hyperspectral sensor to detect oils with sea ice," *Journal of Spectroscopy*, Vol. 2016, 2016.

[14] V. Achard, S. Fabre, A. Alakian, D. Dubucq, and P. Déliot, "Direct or indirect on-shore hydrocarbon detection methods applied to hyperspectral data in tropical area," in *Earth Resources and Environmental Remote Sensing/GIS Applications IX*. International Society for Optics and Photonics, 2018, Vol. 10790, p. 107900N.

[15] N. Abu-Khalaf and M. Hmidat, "Visible/near infrared (vis/nir) spectroscopy as an optical sensor for evaluating olive oil quality," *Computers and Electronics in Agriculture*, Vol. 173, pp. 105445, 2020.

[16] Y. Asano, Y. Zheng, K. Nishino, and I. Sato, "Shape from water: Bispectral light absorption for depth recovery," in *Proc. ECCV 2016*. Springer, 2016, pp. 635–649.

[17] T. Zhi, B. Pires, M. Hebert, and S. Narasimhan, "Multispectral imaging for fine-grained recognition of powders on complex backgrounds," in *Proc. IEEE CVPR 2019*, 2019, pp. 8699–8708.

[18] J. Parkkinen, J. Hallikainen, and T. Jaaskelainen, "Characteristic spectra of munsell colors," *JOSA A*, Vol. 6, No. 2, pp. 318–322, 1989.

[19] A. Lam, A. Subpa-Asa, I. Sato, T. Okabe, and I. Sato, "Spectral imaging using basis lights.," in *Proc. BMVC 2013*, 2013.

[20] S. Han, I. Sato, T. Okabe, and Y. Sato, "Fast spectral reflectance recovery using dlp projector," *IJCV*, Vol. 110, No. 2, pp. 172–184, 2014.

[21] M. Kitahara, T.Okabe, C.Fuchs, and H.Lensch, "Simultaneous estimation of spectral reflectance and normal from a small number of images," in *Proc. VISAPP (1) 2015*, 2015, pp. 303–313.

[22] Ying Fu, Antony Lam, Imari Sato, and Yoichi Sato, "Adaptive spatial-spectral dictionary learning for hyperspectral image restoration," *IJCV*, Vol. 122, No. 2, pp. 228–245, 2017.

[23] H. Hidaka, Y. Monno, and M. Okutomi, "Spectral reflectance estimation using projector with unknown spectral power distribution," in *Proc. CIC 2020*, 2020.

[24] S. Wold, K. Esbensen, and P. Geladi, "Principal component analysis," *Chemometrics and Intelligent Laboratory Systems*, Vol. 2, No. 1-3, pp. 37–52, 1987.

[25] T. Chan and L. Vese, "Active contours without edges," *IEEE TIP*, Vol. 10, No. 2, pp. 266–277, 2001.

[26] J. Jiang, D. Liu, J. Gu, and S. Süsstrunk, "What is the space of spectral sensitivity functions for digital color cameras?," in *Proc. IEEE WACV 2013*, 2013, pp. 168–179.